Analysis of the Current-Voltage Characteristics Lineshapes of Resonant Tunneling Diodes

P. H. Rivera and P. A. Schulz

Instituto de Física Gleb Wathagin, Universidade Estadual de Campinas

13083-970 Campinas, SP, Brazil

Received July 21, 1995

We discuss the influence of a two dimensional electron gas at the emitter-barrier interface on the current-voltage characteristics of a GaAs-AlGaAs double-barrier quantum well resonant tunneling diode. This effect is characterized by the modification of the space charge distribution along the structure. Within the framework of a self-consistent calculation we analyse the current-voltage characteristics of the tunneling diodes. This analysis permits us to infer different tunneling ways, related to the formation of confined states in the emitter region, and their signatures in the current-voltage characteristics. We show that varying the spacer layer, together with barrier heights, changes drastically the current density-voltage characteristics lineshapes. We compare our results with a variety of current-voltage characteristics reported in the literature. The general trend of experimental lineshapes can be reproduced and interpreted with our model. The possibility of tunning tunneling paths is predicted for a range that has not yet been explored experimentally.

I. Introduction

Esaki and Tsu, in 1973, proposed the resonant tunneling diodes[1] of GaAs/AlGaAs. The effect of spatial confinement in these new devices was observed shortly after[2]. Sollner et al[3], in 1983, observed the negative differential resistance of the tunneling diodes at room temperature and open the possibility of technological uses renewing the interest in the field.

Despite many works published in this area, fundamental questions are still open, like the tunneling time and the electron dynamics, due to the fact that the resonant tunneling diodes is an open system out of equilibrium connected to two electronic reservoirs[4].

The use of spacer layers between the heavily doped contacts and barriers permited to get greater peak-to-valley ratios in the current-voltage characteristics of the tunneling diodes. Starting from the coherent tunneling approximation, we systematically analyse the effects of spacer layer, as well as thickness and Al concentration of the barriers on the current-voltage characteristics.

From the coherent tunneling point of view for the analysis of the double-barrier- quantum-well-resonant-tunneling diode, we suppose that the contacts are separately in termal equilibrium, even when the bias voltage is applied to the device[4]. In these circumstances we use the well-known relation of the current density with the applied bias voltage[1,5]:

$$J = \frac{em^*kT}{2\pi^2\hbar^3}\int_0^\infty T(E_z)\ln\left[\frac{1+e^{(\mu-E_z)/kT}}{1+e^{(\mu-E_z-eV)/kT}}\right]dE_z \qquad (1)$$

where $T(E_z)$ is the transmission probability of electrons from the emitter to the collector contacts, μ is the chemical potential of the emitter contact, V is the applied bias voltage, m^* is the effective mass of the conduction electrons defined at the Γ point and E_z is the range of energy for the incoming electrons from the emitter

The transmission probability are obtained from the solution of the Schrödinger equation in the effective mass approximation:

$$-\frac{\hbar^2}{2}\frac{d}{dz}\left(\frac{1}{m^*}\frac{d\Psi}{dz}\right)+\mathbf{E}_c(z)\Psi = E_z\Psi \qquad (2)$$

where z is the crystal growth direction of the semiconducting materials, $m^* = m^*(z)$ is the electron effective mass in different material layers. $\mathbf{E}_c(z)$ is the conduction band profile through the z direction and equal to

$e\Phi + \Delta\mathbf{E}_c^{\Gamma}(z)$, where the first term is the contribution to the potential profile due to the redistribution of charges through the device and the second is given by the conduction band offsets at the interfaces.

Fiig and Jauho[6], suggested to calculate Φ, first semiclassically (Thomas-Fermi approximation) in the contacts and spacer layers regions and quantum mechanically in the accumulation layers and wells. The process is iterative between the Poisson equation:

$$\frac{d}{dz}\left(\epsilon(z)\frac{d\Phi}{dz}\right) = e[N_D^+(z) - n(z)] \qquad (3)$$

and the electron density (Fiig-Jauho model):

$$\begin{aligned} n(z) &= N_c \mathcal{F}_{1/2}\left(\frac{\mu - E_{\|}(z)}{kT}\right) \\ &+ \sum_i kT\rho_{2D}\ln[1 + e^{(E_f-\epsilon_i)/kT}]|\Psi_i|^2 \end{aligned} \qquad (4)$$

where $\epsilon(z)$ is the electrical permitivity, N_D^+ the ionized donor concentration (we suppose that $N_D^+ = N_D$, the donor density), $N_c = \frac{1}{2\pi^2}\left(\frac{2m^*}{\hbar^2}\right)^{3/2}$, $\mathcal{F}_{1/2}$ is the 1/2-th order Fermi-Dirac integral, ρ_{2D} is the 2DEG state density of the accumulation layer and well. ϵ_i and Ψ_i are the energy and wave function of the i-th bound state in the accumulation layer and well. The charge accumulation in the well is weighted by the factor[7], $T_e/(T_e+T_c)$, T_e and T_c are the transmission probabilities through the emitter and collector barrier, respectively.

We calculate the electron density and the conduction band profile iteratively. When the appropiate convergency conditions are satisfied, then the last conduction band profile obtained is used in the equation (2) to calculate the transmission probability, which is used in the equation (1) to obtain the current density through all device. This process is repeated for each applied bias voltage. We consider for all calculations a well of GaAs of 50 Å and barriers of $Al_xGa_{1-x}As$ of 25 Å (for $x = 0.3$, the $\Delta\mathbf{E}_c^{\Gamma} = 0.258$ eV and for $x = 0.57$, $\Delta\mathbf{E}_c^{\Gamma} = 0.507$ eV, [8],[9]), donor concentration in the contacts are $1 \times 10^{18}/\text{cm}^3$ and the Fermi energy associated is 0.054 eV.

We start by discussing a single barrier device. It has two contacts and two symmetric spacer layers of 600 Å. With applied bias voltage an accumulation layer is formed at the interface of the barrier (emitter side) leading to formation of bound states. The first starts to be bounded at 0.02V and the next at 0.05V, Fig. 1.a. When the potential bump formed by the spacer layer is above the Fermi level (low bias), there are resonant tunneling channels through the first and the second bound states. This 3D-2D-3D tunneling channel is very weak with respect to the 3D-3D channel through the barrier when the potential bump is below the Fermi level, Fig. 1.b. From 0.2V up the potential bump remains fairly constant, the 3D-3D tunneling channel predominates and the current density shows Fowler-Nordheim like oscilations.

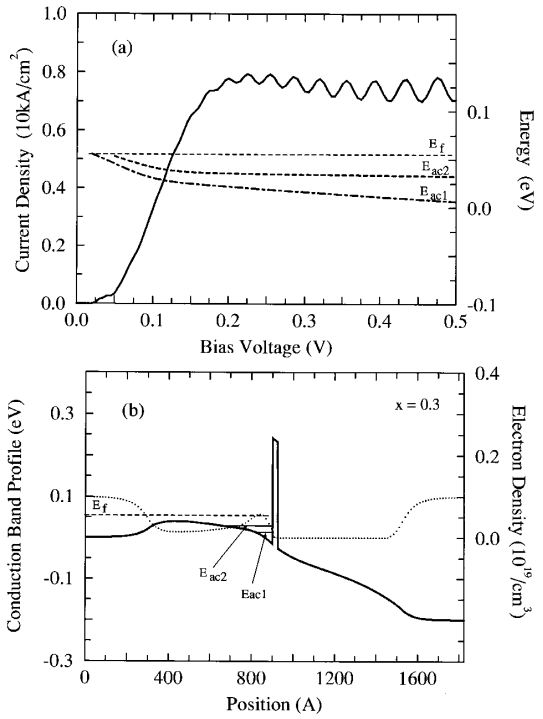

Figure 1. (a) The current density (solid line) of a single barrier device with spacer layer vs applied bias. The variations of the energies of quasi-bound states, E_{ac1} (dot-dashed) and E_{ac2} (dashed), are also indicated, as well as the position of the Fermi energy, E_f (thin dashed). (b) The conduction band profile (solid line) and the electron density (dotted) vs position.

We proceed by studying now a double barrier structure. Here we consider the same parameters describing the contacts, spacer layers, as well as barrier thickness. Now the barriers are separated by a 50Å GaAs QW. Our interest will concentrate on the effect of barrier height variation on the tunneling characteristics. In Fig. 2 we show a device with 30% of Al in the barriers. In the accumulation layer there are two quasi-bound states, but these do not show related features in the J-V characteristic as can be seen in Fig. 2.a. This J-V

curve has a maximum due to the predominant 3D-2D-3D tunneling channel above the potential bump. The potential profile for a bias near the resonance condition is shown in Fig. 2.b.

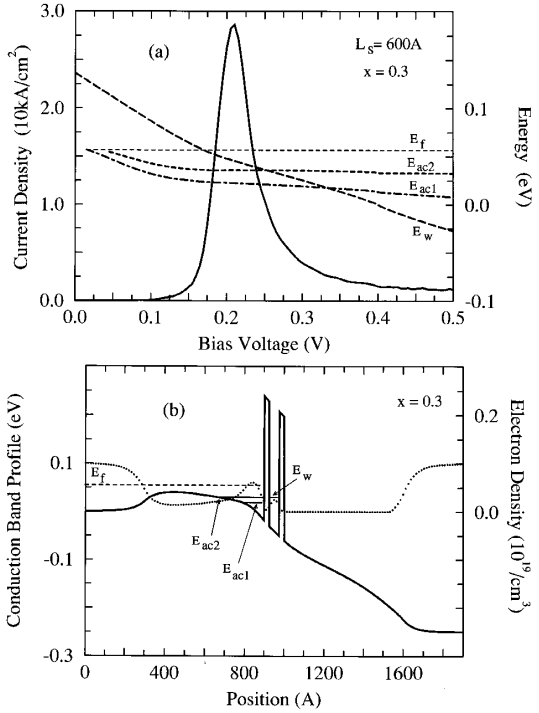

Figure 2. (a) The current density (solid line) of double barrier quantum well device vs applied bias. The variations of the quasi-bound states, E_{ac1} (dot-dashed), E_{ac2} (dashed), of the accumulation layer and the quantum well level, E_w (long dashed) with applied bias are also shown. (b) The conduction band profile (solid line) and the electron density (dotted) vs position. The position of the Fermi energy, E_f, is also indicated in (a) and (b).

For a device with 57% of Al in the barriers, Fig. 3, the second quasi-bound state (2DEG) in the accumulation layer, E_{ac2} and the well state (2DEG), E_w, couple strongly. This effect modifies completely the line shape of the J-V characteristics, giving rise to a second resonance peak, characterizing a 3D-2D-2D-3D tunneling path. Indeed, in Fig. 3.a the position of the second peak in the J-V curve coincide with the anticrossing of the above mentioned states, $\mathbf{E}_w$ and E_{ac2} This tunneling channel predominates with respect to 3D-2D-3D tunneling channel[10]. Fig. 3.b shows the potential profile as a function of position for a bias value near the first resonance in the J-V curve, namely the 3D-2D-3D tunneling path.

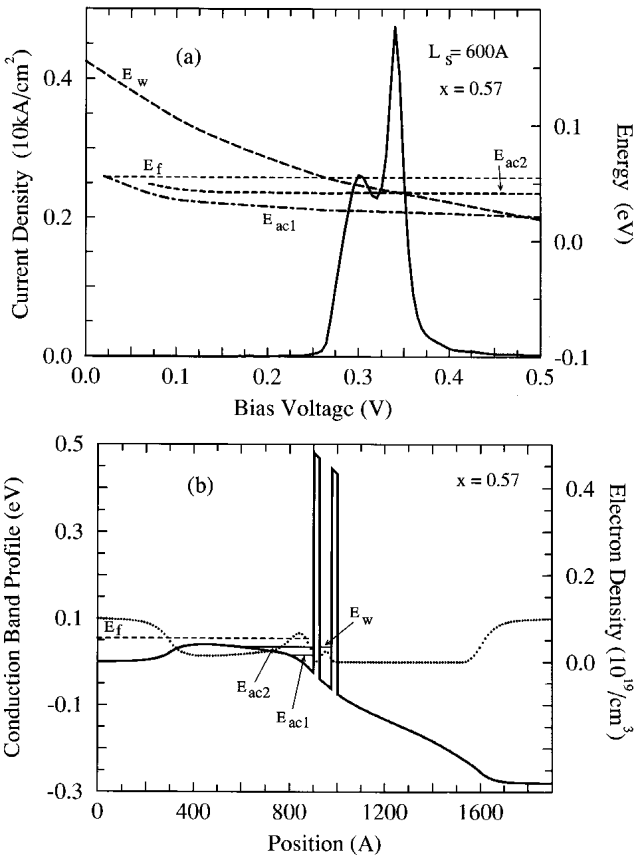

Figure 3. (a) The current density (solid line) of double barrier quantum well device vs applied bias. The variations of the quasi-bound states, E_{ac1} (dot-dashed), E_{ac2} (dashed), of the accumulation layer and the quantum well level, E_w (long dashed) with applied bias are also shown. (b) The conduction band profile (solid line) and the electron density (dotted) vs position. The position of the Fermi energy, E_f, is also indicated.

Our next step is to verify the effect on the tunneling current of the barries asymmetry[11,12]. For this purpose we consider 57% of Al in the barriers, a 50Å well width, a 300Å spacer layer and the same donor concentration in the contacts as in the previous cases. We found that the J-V characteristics are very sensitive to the barrier thickness asymmetry. In Fig. 4.a the emitter barrier thickness is varied from 25 to 40Å, keeping the collector barrier constant (25Å). We can see that the 3D-2D-2D-3D tunneling channel predominates with respect to the 3D-2D-3D tunneling channel when the emitter barrier becomes thicker. In Fig. 4.b the collector barrier thickness is varied along the same parameters of the Fig. 4.a. (while keeping now the emitter barrier tickness constant). Here the modification of the tunneling current characteristics is completely different from the former case and no consideration on predom-

inancy of tunneling paths with increasing asymmetry can be stated.

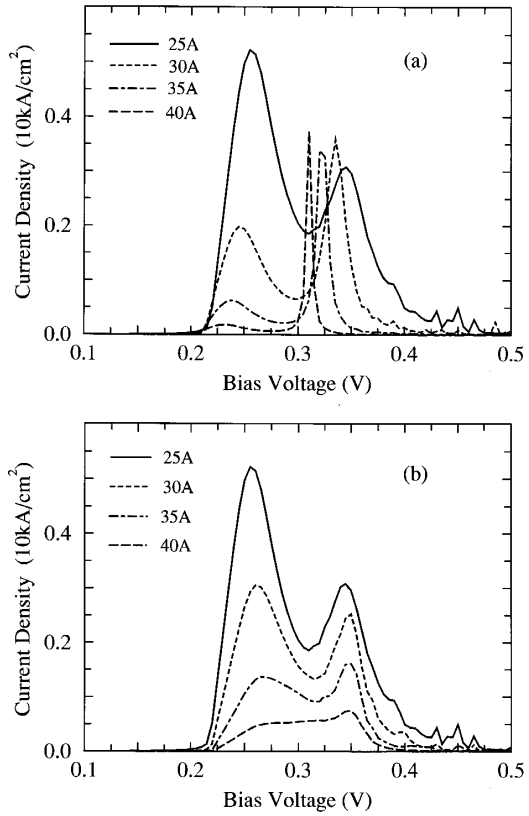

Figure 4. The current densities of double barrier quantum well devices vs applied bias. Different thicknesses of one of the barriers: 25Å (solid line), 30Å (dashed), 35Å (dot-dashed) and 40Å (long dashed). (a) When the emitter barrier is varied and collector barrier is 25Å thick. (b) When the collector is varied and emitter barrier is 25Å thick.

The main conclusion is that one has two limits for the lineshape of the current density- voltage characteristics. The first one corresponds to a single highly asymmetric peak, abrupt at the lower bias side, due to tunneling of 3D electrons over the potential bump in the spacer layer. The second limit shows a doubly peaked structure, where the second is due to the coupling of the quasi-bound states in the accumulation layer and double-barrier quantum well. The difference between these two limits is not only due to the charge accumulation but a compromise of various effects, namely the effective transparency of the collector barrier, pinning of the accumulation layer level and the width of the energy window between the Fermi energy and the top of the potential bump in the emitter region. These effects could be seen on one sample with asymmetric barriers by simply changing the bias polarity. This is suggested by the results shown in Fig. 4. There are some evidences of these effects in experimental results[11,12], although not conclusive. For the device parameters considered here, the main experimental problem concerns the high currents due to the very thin barriers.

References

1. R. Tsu and L. Esaki; Appl. Phys. Lett. **22**, 562 (1973).
2. L. L. Chang, L. Esaki and R. Tsu; Appl. Phys. Lett. **24**, 593 (1974).
3. T. C. L. Sollner, W. D. Goodhue, P. E. Tannenwald, C.D. Parker and D. D. Peck; Appl. Phys. Lett. **43**, 588 (1983).
4. W. R. Frensley; Phys. Rev. **B 36**, 1570 (1987) - Rev. Mod. Phys. **62**, 745 (1990).
5. C. B. Duke; *Tunneling in Solids*, Supplement 10 - Solid State Physics, F. Seitz, D. Turnbull and H. Ehrenreich Eds.; Academic Press, New York (1969).
6. T. Fiig and A. P. Jauho; Appl. Phys. Lett. **59**, 2245 (1991) Surf. Sci. **267**, 392 (1992).
7. F. W. Sheard and G. A. Toombs; Semicond. Sci. Technol. **7,** B460 (1992).
8. S. Adachi; J. Appl. Phys. **58**, R1 (1985).
9. M. Rossmanith, K. Syassen, E. Bockenhoff, K. Ploog and K. von Klitzing; Phys. Rev. **B 44**, 3168 (1991).
10. P. H. Rivera and P. A. Schulz; Appl. Phys. Lett. **67**, 2675 (1995).
11. A. Zaslavsky, V. J. Goldman, D. C. Tsui and J. E. Cunningham; Appl. Phys. Lett. **53**, 1408 (1988).
12. M. Tewordt, L. Martín Moreno, J. T. Nicholls, M. Pepper, M. J. Kelly, V. J. Law, D. A. Ritchie, J. E. F. Frost and G. A. C. Jones; Phys. Rev. **B 45**, 14407 (1992).